Earth's inner core: revealing the structures behind the PKP core phase triplication

N.A. Blom –[1] supervisors: A.F. Deuss,[2] H. Paulssen,[1]

The PKP core phase triplication and strong precursors to inner core phase PKIKP cause problems in studying structures at ∼100-200 km depth beneath the ICB, hindering an accurate discussion of deeper structures. Here, we stack seismograms in slowness and time to separate the PKP phases that arrive simultaneously, but with different slowness. We use these stacks to study the inner core between ∼100 and 380 km beneath the ICB in the Western hemisphere of the inner core, a region with anomalously strong anisotropy. Our data is in accordance with shallow anisotropy < 100 km beneath the ICB. Moreover, it reveals a marked increase in seismic velocity over the depth range investigated, up to a maximum of ∼5% faster than the reference model AK135. Such strong anisotropy has not been demonstrated before at these shallow depths.

1. Introduction

Given its remoteness and small size (less than 1% of the Earth's volume), the inner core plays a surprisingly important role in the Earth's dynamics. Only discovered in 1936 [*Lehmann*, 1936], it is still relatively unknown, although many enigmatic characteristics have come to light over the past few decades. It has been found to be anisotropic, with the axis of symmetry approximately along the Earth's rotation axis and rays in the polar direction travelling faster than those in the equatorial plane (*Morelli et al.* [1986], *Woodhouse et al.* [1986]). More recently, it was discovered to consist of two seismically distinct hemispheres (*Tanaka and Hamaguchi* [1997], *Deuss et al.* [2010]) which are separated by sharp boundaries [*Waszek and Deuss*, 2011]. The hemispheres themselves are not homogeneous either, as both isotropic and anisotropic velocities are found to vary with depth.

A wealth of different mechanisms has been proposed to explain both the anisotropy and the existence of hemispheres, all leading back to the question of how the inner core interacts with its surroundings. While some propose that the anisotropy is frozen into the inner core as it solidifies (*Karato* [1993], *Bergman* [1997]), another hypothesis is that it is formed later on, as a result of thermal convection [*Jeanloz and Wenk*, 1988] or magnetic field stresses [*Karato*, 1999]. Whatever the mechanism, it also has to explain the existence of hemispheres and any other variations inside the inner core, with depth or laterally.

In order to be able to determine what processes govern this remotest part of the Earth, it is important to have an accurate idea of the structures inside it. Large steps towards this goal have been taken in recent years, with the compilation of large sets of inner core body wave and normal mode data. Both methods have their own merits, but while modes have the advantage of uniform coverage, they are long period data and have limited depth resolution. Here, we are interested in a more accurate idea of the detailed structures, for which body waves are more suitable.

The upper ∼100 km of the inner core has been studied in relatively much detail. It is generally agreed that the isotropic velocity of the Eastern hemisphere is higher than that of the Western hemisphere (*Tanaka and Hamaguchi* [1997], *Waszek and Deuss* [2011]) while the Western hemisphere is much more anisotropic than the Eastern hemisphere (3% as opposed to 0.5-1%) (*Tanaka and Hamaguchi* [1997], *Creager* [1999], *Irving and Deuss* [2011], *Waszek and Deuss* [2011]) An isotropic layer has been found at the top of the Western hemisphere (*Shearer* [1994], *Song and Helmberger* [1995]) which is thought to be about 60 km in thickness. Below this, anisotropy increases abruptly to 2.8% [*Waszek and Deuss*, 2011]. Some studies also suggest a layer of high (isotropic) velocity at the top of the Eastern hemisphere (*Cormier* [2007], *Waszek and Deuss* [2011])

Much more uncertainty and variation is found in the deeper regions of the inner core. Suggested values for anisotropy in the Western hemisphere vary highly from 2-4% at depths of 100-200 km beneath the ICB (*Creager* [1999], *Sun and Song* [2008]), to 8% at depths >250 km [*Song and Xu*, 2002]. The Eastern hemisphere is found to be more isotropic, but it has been suggested (e.g. *Irving and Deuss* [2011]) that anisotropy may increase with depth, which could mean that hemispherical differences may disappear at depth.

At epicentral distances of 130-143°, PKiKP and PKIKP can be used to study the inner core up to ∼100 km depth. And at 148-155°, PKPbc, PKPab and PKIKP can be used to study the inner core beneath ∼300 km. An unfortunate geometry of raypaths around 145° causes intermediate depths to remain seismically hidden, which consequently also makes uncertainties at depth larger (see Figure 1). Here, the core phases PKPab, PKPbc, PKiKP and PKIKP all arrive at approximately the same time – a result of the lower velocity outer core in between the higher velocity inner core and mantle. These intersecting rays, plus strong precursors to PKP at lower epicentral distances, make it impossible to recognise individual phases in the seismogram at about 140-150° epicentral distance.

This is very unfortunate, because as a result, a whole spherical shell near the inner core boundary remains invisible to direct scrutiny. As long as the seismic structures there remain unknown, deeper regions cannot be defined accurately either. Depending on assumptions about the thickness and velocity structure of this layer, travel times through the whole inner core can vary by up to 1 s. Considering that the total size of travel time deviations for polar paths in the deeper inner core are around 3-5 s (see for example *Irving and Deuss* [2011] figures 3 and 5), it is actually quite essential that this layer is accounted for properly and accurately. In this study, we will bridge the gap between 143° and 148° by stacking seismograms in this range of epicentral distances in slowness and time, attempting to separate the PKP core phases and measure inner core differential travel times.

[1]Department of Earth Sciences, Universiteit Utrecht, The Netherlands

[2]Department of Earth Sciences, University of Cambridge, United Kingdom

0094-8276/13/$5.00

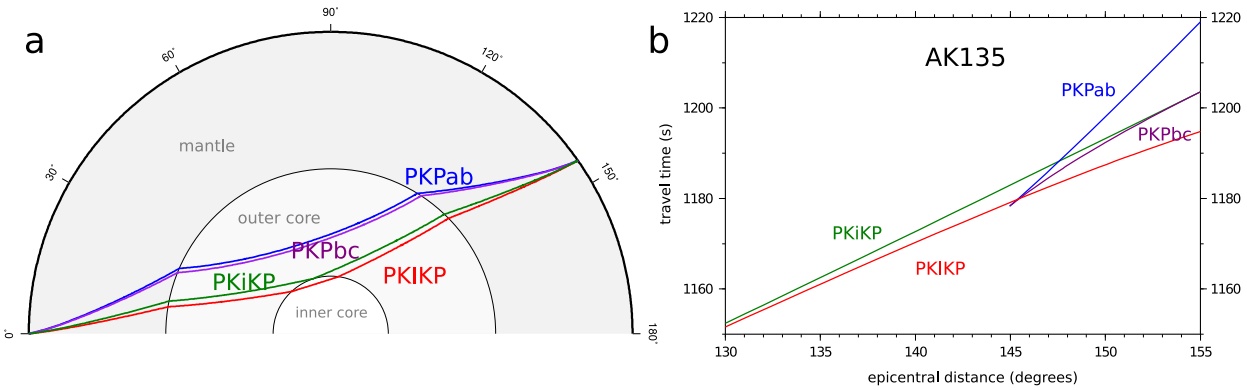

Figure 1. (a) Ray paths of the different compressional seismic phases that pass through the core. PKIKP (red) passes through the inner core, PKiKP (green) reflects off the inner core boundary, PKPbc (purple) passes through the deep outer core, and PKPab (blue) passes through the shallower outer core. (b) Travel times of the same phases at epicentral distances of 130-155°. Predictions are calculated using TauP [*Crotwell et al.*, 1999] for model AK135 [*Kennett et al.*, 1995]. Around 145° we see that the phases arrive so closely together that they cannot be identified separately (see Figure 2).

2. Methods

We study the inner core using PKIKP (also called PKPdf), a compressional seismic body wave which travels through the mantle, the outer core and into the inner core (Figure 1a). As a reference phase PKiKP is used, which travels nearly the same path but reflects off the boundary of the inner core instead of entering it. The other PKP phases are PKPab and PKPbc, which travel through the mantle and outer core only. Because PKIKP and PKiKP paths travel so closely together, heterogeneities encountered along the way will affect both rays in nearly the same way. Likewise, a possible mislocalisation of the hypocentre will have nearly the same effect on both phases. A discrepancy between the actual differential travel time and the model prediction can therefore be considered a result of inner core structure.

Direct identification of the phases in the seismograms is not possible because of the triplication at 145° epicentral distance. We therefore stack bins of seismograms in slowness and time. This technique, called the Velocity Spectral Analysis (or Vespa) method, enables us to separate seismic arrivals both in terms of time and slowness [*Davies et al.*, 1971]. Seismic traces are stacked for a range of slownesses, which results in a plot (called vespagram) of signal amplitude versus slowness p and travel time t. As long as a phase's slowness remains approximately constant within a stack, its energy will add up constructively. As a result, phases that arrive at the same time but with different slownesses can be identified separately. It was immediately realised that this method was especially suitable to study core phases (*Davies et al.* [1971], *Doornbos and Husebye* [1972]), and we will apply it here to separate PKIKP and PKiKP from PKPab and PKPbc.

Efficient analysis of seismic signals needs to strike a balance between suppressing noise and enhancing possibly weak signals. A very efficient method to this end is the Phase Weighted Stack or PWS) technique [*Schimmel and Paulssen*, 1997], which uses the phase coherency across the stacked traces as an additional weighting measure. The main advantage of this technique is that it suppresses incoherent noise, while maintaining the waveforms of the stacked signals (unlike other stacking techniques).

3. Data

We focus on polar paths in the Western hemisphere, whose travel times are known to be anomalous because of the generally strong anisotropy in this part of the inner core. Polar paths are defined as paths for which the angle between the Earth's rotation axis and the path at its turning point, ζ, is smaller than $\zeta < 35°$. Events are selected on location – they must yield polar paths – and magnitude. Recordings from South Sandwich Islands events to stations mainly in northwest Canada and Alaska are abundant and are therefore suitable for our aims. All used events are around magnitude $M_W = 6$ and at depths up to 200 km (see Table 1).

Seismic traces were gathered from the IRIS database and the Canadian National Seismograph Network. They were filtered around 1 Hz, checked for quality, resampled at 10 s^{-1} and binned in 5° bins for each event. Any bins that con-

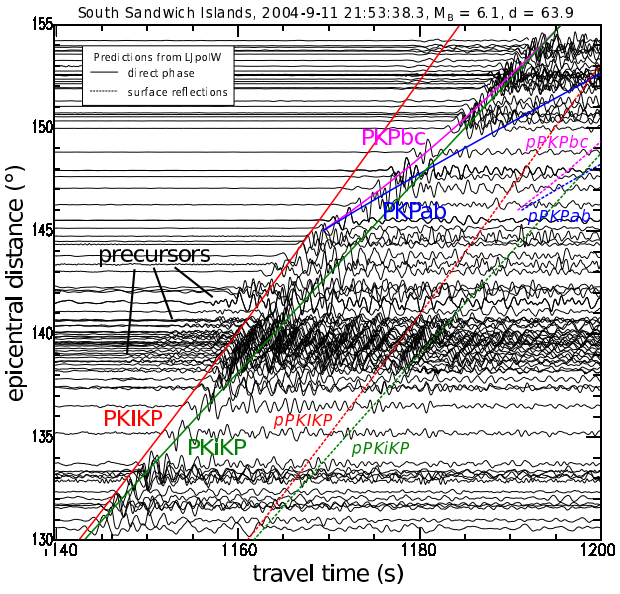

Figure 2. Seismograms through the inner core's Western hemisphere in the polar direction ($\zeta < 35°$), filtered around 1 Hz. Predictions for the arrival times are shown as solid lines (direct phases) and dotted lines (surface reflections), calculated for model LJpolW, the inner core velocity model for polar paths in the inner core's Western hemisphere [*Waszek and Deuss*, 2011].

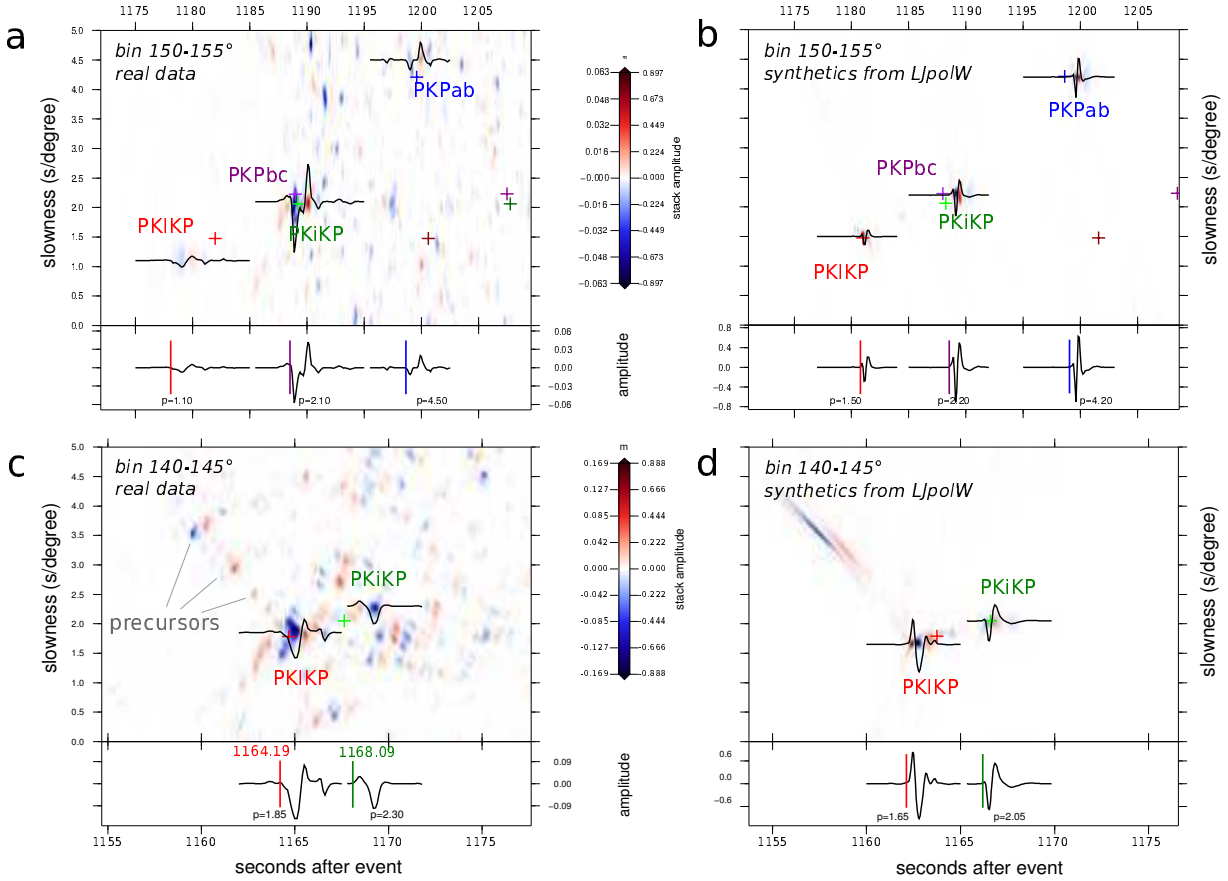

Figure 3. Vespagrams produced using the Phase Weighted Stacking technique with $\nu = 3$ (see *Schimmel and Paulssen* [1997]). Shown here are stacks of the bin 150-155° (a,b), and of the bin 140-145° (c,d). (a) and (c) are vespagrams for the real data, (b) and (d) for synthetics processed in the same way. Model predictions for direct phases and surface reflections, made with TauP for model AK135 [*Kennett et al.*, 1995], are plotted as + symbols. The colour scheme is the same as in Figure 2 where the darker colours signify surface reflections. The streaked feature in (d) is a result of boundary effects in WKBJ, made visible because of the Phase Weighted Stack [*Schimmel and Paulssen*, 1997].

tained less than 4 traces were discarded. The traces were normalised and stacked at slownesses ranging from 0 to 5 s/° using the Phase Weighted Stack. The stacks are centred at the station in the bin with the median epicentral distance, a crude but effective method to ensure that the differential travel time is calculated at the distance where most of the data is found. This also ensures that the resulting vespagram does not become distorted as a result of unbalanced trace distribution within the bin.

Phases are picked by comparing the arrivals in the observed vespagrams to predictions from AK135, and differential travel time residuals are calculated with

$$R = (t_{\mathrm{PKiKP}} - t_{\mathrm{PKIKP}})_{\mathrm{data}} - (t_{\mathrm{PKiKP}} - t_{\mathrm{PKIKP}})_{\mathrm{model}} \quad (1)$$

Residuals are initially calculated with respect to velocity model AK135 [*Kennett et al.*, 1995], which is designed to provide a good fit to a wide range of phases, and which is especially suitable for studying the core. Model travel times are calculated using TauP [*Crotwell et al.*, 1999].

4. Results

As we can see in Figure 2, it is impossible to separate the PKP phases around 145°, both because of the simultaneous arrivals and the PKP precursors, which become more and more pronounced towards 145° epicentral distance. To stack the seismograms, we therefore divide them into epicentral distance bins of 5° width: 140-145°, 145-150°, 142.5-147.5° and 150-155°. Figure 3 shows vespagrams for two of these bins for the same event. The red and blue colours represent positive and negative stacked amplitudes, respectively. Crosses plotted on top represent model predictions for the arrival time and slowness of each of the phases.

As a proof of concept, we first compare vespagrams for real and synthetic data between 150° and 155° (Figure 3a,b). The data are from a South Sandwich Islands event of 11 September 2004 (21:53:38.3, $m_b = 6.1$, depth = 63.9 km). Synthetic seismograms (Figure 3b) are calculated for the exact same source parameters and station locations, and are processed in the same way. The vespagram for synthetic data shows sharp and concentrated peaks for each of the PKP phases at the predicted arrival time and slowness. PKPbc produces the strongest amplitudes while PKIKP is fainter – again in accordance with expectations (see also Figure 2). PKiKP cannot be distinguished from PKPbc at these distances, as it arrives not only simultaneously but also with the same slowness.

The real data (Figure 3a) results in a plot which is somewhat less clear, with several more arrivals at a whole range of slownesses, especially after the arrival time of PKPbc. The PKP phases do however stand out clearly: especially PKIKP and PKPbc are easily identified. PKPbc and PKPab both

arrive very close to their predicted slowness and arrival time. PKIKP, however, deviates from the predictions. Not only is the signal much more smeared out (indicating high attenuation in the core), it arrives both earlier and at smaller slowness than expected. This is in line with our expectations for polar paths in the Western hemisphere, which have been studied before at these distances (e.g. *Irving and Deuss* [2011]). The small slowness indicates that the ray bottoms at a deeper point inside the inner core than predicted. This is a robust signal over the whole range of 25 seismograms and 5°. Furthermore, the waveforms substantially match our expectations.

Next, we investigate the epicentral distance range of 140-145°, which is where the PKP triplication occurs. From the original seismograms (Figure 2) it is clear that, while trends are sometimes visible over a range of seismograms, it would become very tricky indeed to pick PKIKP and PKiKP from the individual seismograms in this range. The onset of PKIKP is obscured by PKP precursors. In the synthetic seismograms (Figure 3d) we see that PKIKP and PKiKP are very well separable. While these synthetics contain no precursors, we can conclude here that at least the effect of the triplication can clearly be circumvented by stacking. The vespagram from real data contains more noise, but is still very clear. The two principal phases can be recognised as PKIKP and PKiKP. They have opposite polarities – exactly as we would expect. Both phases are slightly early with respect to their predictions, although PKIKP more so. In this bin, PKIKP is a sharper signal than in the bin 150-155°. Generally, we see that PKIKP becomes increasingly diffuse with depth, a result of attenuation. Arrival times are picked at the first up/down at the slowness containing the largest amplitudes for that particular phase.

A line of smaller arrivals is visible starting at PKIKP and moving to higher slownesses and earlier arrivals: these are the precursors which are also clearly visible in the original seismograms (Figure 2). When we measure the slowness and arrival times of the precursors in the original seismograms, they do in fact correspond closely to the values determined from this vespagram. [1]

Results for the distance bins of 145-150° and 142.5-147.5° were produced and analysed in much the same way. PKPbc is usually the most pronounced phase, with PKPab next and PKIKP and PKiKP mostly rather faint. Especially PKiKP becomes small as we go to higher epicentral distance. It is however still visible in both bins and distinguishable from PKPbc, an important result because it enables us to use PKiKP-PKIKP differentials up to a greater distance than has previously been done. PKIKP becomes more diffuse with depth, again indicating increased attenuation. PKIKP arrives earlier and at lower slowness as we go deeper, confirming the trend we also see 150-155° and 140-145°.

We investigated a total of 30 events. 16 of these (Table 1) were used to measure differential travel times, resulting in 9 differentials for the bin 140-145°, 8 differentials at 145-150° and 4 differentials at 142.5-147.5°. This relatively high rejection rate is a result of quality requirements – both phases must be clearly distinguishable in the vespagram – and of the fact that some bins simply did not contain enough seismograms for stacking.

Residuals (Equation 1) for all bins and events are plotted in Figure 4, with in red those calculated with respect to AK135. Only residuals from non-overlapping data bins are plotted. Residuals are plotted at the epicentral distance at which the stack has been centred, and the vertical bars indicate the width of the stack, which is variable according to the exact spread of stations that were available. The general trend is that residuals become larger with increasing epicentral distance, which is also deeper in the inner core. This trend is visible over the different bins, but also within the bins as a result of the data distribution within bins, and means that greater velocities are needed at depth.

Table 1. Earthquakes used in this study[a]

Event date & time (UTC)	Magtype & mag	depth (km)
2004-9-6 14:17:19.3	M_W= 5.8	10.0
2004-9-11 21:53:38.3	M_B= 6.1	63.9
2004-10-8 15:28:39.2	M_W= 5.9	101.5
2004-10-26 22:53:07.8	M_W= 6.2	10.0
2004-11-7 02:41:41.0	M_W= 5.8	38.6
2005-5-18 09:10:53.6	M_W= 6.0	102.2
2005-6-12 19:26:24.8	M_W= 6.0	94.1
2005-7-25 19:45:16.0	M_B= 5.5	84.8
2005-8-4 12:11:21.3	M_O= 5.5	45.9
2005-9-9 19:55:21.8	M_W= 5.6	142.8
2006-5-29 05:20:48.4	M_O= 5.6	124.4
2008-4-14 09:45:19.7	M_W= 6.0	140.2
2010-12-8 05:24:35.2	M_W= 6.3	29.4
2011-8-21 12:38:53.7	M_W= 5.6	130.4
2011-9-3 04:48:57.3	M_W= 6.4	84.0
2011-12-11 09:54:55.2	M_W= 6.2	116.0

[a] All earthquakes are from the South Sandwich Islands

5. Interpretation

This is the first study where PKIKP-PKiKP differentials are measured at distances of 143-150° – and therefore so deep into the Earth's inner core. Because the paths are so close, the effect of mantle heterogeneities is filtered out without even applying corrections to the travel times. We compare the produced differential travel times to predictions for various models and calculate the residuals. For model AK135, positive residuals between 0.5 and 5 s are found with the lowest residuals at lowest epicentral distances (and therefore shallow in the inner core) (see Figure 4). There is a clear trend of residuals becoming larger as we go to higher epicentral distances (or deeper into the inner core). This is not surprising as AK135 does not take into account any anisotropy in the inner core.

Next, we use the polar Western model from *Waszek and Deuss* [2011] (LJpolW), which takes into account shallow anisotropy of the inner core and goes down to a depth of 100 km beneath the ICB. The top 60 km of the inner core has an isotropic layer, after which anisotropy increases sharply to 2.8% (*Song and Helmberger* [1995], *Waszek and Deuss* [2011]). We compare our data to two versions of this model. If we let velocities drop back to AK135 values immediately at 100 km, our data at low epicentral distances produce much lower residuals for LJpolW than for AK135, indicating that there is indeed a good fit with shallow data. At larger epicentral distances however, the residuals are still equally off. If instead we extend the higher velocity of 11.33 km/s from LJpolW all the way into the inner core, the residuals become a little lower, the maximum value dropping to ∼2 s. The trend of larger residuals at larger distances is however still clearly present, which means that the maximum anisotropy of 2.8% is not sufficient.

We can now determine the requirements for an improved model. Model LJpolW explains our data up to 100 km into the inner core. Deeper down, a gradual increase in velocity is the most logical choice given the gradual trend seen in our data. Because we stack over a range of 5°, this gradual trend is to be expected: any sharp interface would be smoothed over the bin. Figure 4a shows the model (NpolW) which gives the fit to the data in terms of residuals, which

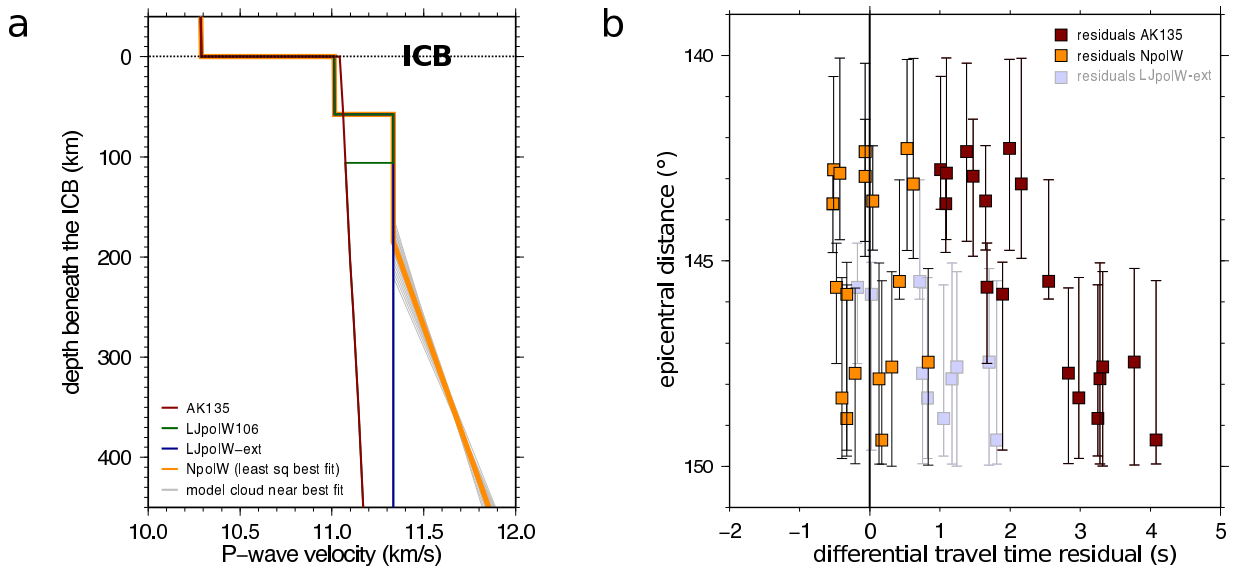

Figure 4. (a) Velocity models used in this study. Model NpolW is the least squares minimum residuals model generated using PKIKP-PKiKP differential travel times obtained in this study. The sum of squares is 2.99 s for this model, while the models plotted in grey are those models closest to the minimum, with sums of squares <3.25 s. (b) Differential travel time residuals for our data, calculated for models AK135 (red), NpolW (yellow), and LJpolW-ext (light blue). While the residuals for AK135 and LJpolW-ext clearly increase with increasing epicentral distance, those for model NpolW remain close to zero for the whole range of epicentral distances.

are plotted in Figure 4b. Model NpolW has been calculated using a least squares method for the residuals. The tested models varied in depth at which the gradual increase in velocity started, and velocity gradient over the region of increasing velocity. The minimum sum of squares for model NpolW is 2.99 s, and plotted in grey around model NpolW are the models with residuals <3.25 s.

Our model shows that the level of anisotropy at shallower depths (2.8% between 60 and 100 km below the ICB according to *Waszek and Deuss* [2011]) is not sufficient to explain our data. Previously found anisotropy is mainly seen as anomalously early polar paths: equatorial results, both at lower and higher epicentral distances, are much closer to model predictions. We have also found early polar paths, leading to an increase in polar velocities, which we interpret as a further increase in anisotropy to 5.4%. This value is similar to what has been found in earlier studies. It is slightly higher than values found using PKIKP-PKPbc residuals in [*Irving and Deuss*, 2011] for epicentral distances >150°, which is probably a result of the fact that their residuals are averaged over the whole upper inner core, which also includes the upper isotropic layer.

6. Discussion

While this layer is not very thick, it is important that its structures are accounted for properly: travel times for even the deepest paths through the inner core (with the shortest route through this layer) vary by up to 1 s depending on the velocity structures chosen for this single layer. Our understanding of the inner core as a whole therefore benefits from more accurate knowledge about this shallow layer.

Our results shed further light on the discussions about the development of anisotropy inside the inner core. Below the 60 km thick isotropic layer, we find that anisotropy in the Western hemisphere of the inner core smoothly increases with depth. Although results become less accurate as we go deeper, other studies seem to confirm this trend. An abrupt change in anisotropy would mean different processes acting at different depths or times, but we find no evidence for this. It then seems probable that the process responsible for the anisotropy is gradual or constant. One type of process that would fit our observations is a post-solidification process (such as thermal convection [*Jeanloz and Wenk*, 1988] or due to magnetic field stress [*Karato*, 1999]) which acts on the whole inner core. Deeper layers, which have been solid for a longer time, would then be more anisotropic.

We have studied the inner core using events from the South Sandwich Islands, and stations located in northwest Canada and Alaska. Although the sampling of the Western inner core is therefore not complete, the raypaths that we study do extend laterally over about 30° which corresponds to ∼600 km near the ICB. Moreover, we see this increasing velocity trend over a whole range of depths into the inner core, while similar results for paths away from the Americas have been reported as well [*Waszek and Deuss*, 2011].

The method that we have developed here can be applied to any event which has a suitably dense spread of stations between 140-150°. Thus far, we have only studied polar paths in the Western hemisphere. The addition of equatorial paths and data for the Eastern hemisphere will help us to get a more complete understanding of the anisotropy in this region. If the density of stations is high enough, it would become possible to calculate the full anisotropy as a function of ζ. In the case of a suitably high station density, smaller bins might also be attempted. Our bin size was mainly governed by the amount of traces needed for a workable stack: high-density arrays could produce much more condensed data. Finally, incorporating corrections for heterogeneities beneath the stations or in the mantle could possibly improve the quality of the vespagrams. While the differentials for PKiKP-PKIKP will not be affected much as the phases travel so closely together, the coherency across different traces in the same stack will increase, which could make phases easier to pick.

A more rigorous study of the range of epicentral distances between 140° and 150° helps to get a better grip on deeper

structures as well. This may help us to answer outstanding questions, both about the extent and origin of anisotropy at depth and the existence of hemispheres. *Waszek and Deuss* [2011] have shown that the hemisphere boundaries move to the east with depth – the question is then: does this pattern continue beneath 100 km or do the boundaries remain in place?

7. Conclusion

Stacking, commonly used for mantle phases, has been shown to also be a useful technique to differentiate between simultaneously arriving core phases. Smaller phases such as PKiKP, which are hidden in the coda of the bigger PKPbc and PKPab phases, can be distinguished, as well as precursors to PKIKP, which have a clearly defined, separate signal.

We have used the stacking techniques to separate the PKP phases around the triplication at 145° epicentral distance and have thus been able to study the region of ∼100-200 km depth beneath the ICB, which had hitherto remained invisible. In the Western hemisphere, we find that anisotropy increases gradually beneath the 60 km thick isotropic upper layer. A gradual increase in anisotropy with depth fits with a post-solidification process as a cause of anisotropy in the inner core.

Appendix A: Precursors

A1. Introduction

In this study we encountered one event (South Sandwich Islands, 11 September 2004 m_b = 6.1, depth = 63.9 km) which features a remarkably regular set of precursors to PKIKP. These are visible at stations in northwestern Canada and Alaska around ∼140° epicentral distance, over a range of several degrees. The precursors have a fan shape with slownesses ranging from that of PKPab to that of PKIKP (see Figure 2). This regularity and the different slownesses, which are clearly visible by eye in the seismograms, set the event apart from others, as a result of which we feel it merits some discussion of its own.

Precursors (and especially those to PKIKP) have received considerable attention since the 1970s (e.g. *Doornbos and Husebye* [1972]). Nowadays, they are mostly thought to originate from heterogeneities in the mantle which scatter the seismic signal. They are studied both on a global, statistical scale (*Hedlin et al.* [1997], *Margerin and Nolet* [2003]) and on a local scale, focussing on specific events or regions of events (e.g. *Wen* [2000], *Niu and Wen* [2001], *Cao and Romanowicz* [2007], *Thomas et al.* [2009]). Results of the global studies indicate that heterogeneities are probably very abundant throughout all of the mantle, with a typical size of ∼8 km [*Hedlin et al.*, 1997]. Here, we will analyse the set of precursors in our event, and try to locate one specific precursor which is particularly well-developed and clear.

A2. Methods

Several previous studies have devised methods to study and locate precursors. They often make use of seismic arrays in order to try to constrain the location of specific scatterers in the mantle. We will follow a similar approach, but instead of limiting ourselves to specific arrays, we make use of any station in the region which displays the precursor.

Wen [2000] and *Niu and Wen* [2001] used a (tomographical) approach with arrays situated around 120-140° from an earthquake-prone region. They combined the onset times of precursors for all the different stations and of several events to determine the most probable location of the scatterer. This was done by performing a grid search at different depths above the CMB. Their method assumes that all the precursor signal is a result of one and the same scatterer.

A different method was adopted by *Cao and Romanowicz* [2007] who tried to locate scatterers in the mantle by analysing the slowness and back-azimuth for distinct precursors using the Vespa method. Based on ray tracing and the assumption that rays are only scattered once, these values, together with travel time, give approximate locations for the scatterers. We use an approach which is similar to that of *Cao and Romanowicz* [2007], but assume that the scatterer has the same back-azimuth as the source, i.e. that it is located in the plane of source, receiver and centre of the earth. This means that we only determine the apparent slowness in this plane. As we shall see later on, this assumption does not affect our results in a strong way.

The precursors we are interested in are visible by eye in the original seismograms of the given event (see Figure 2). They are very clear between ∼138-141°, and we will therefore stack the seismograms in this range to produce vespagrams (see Figure 6). We create vespagrams for the seismograms as they are, as well as for a set where all traces have been realigned with respect to picks of PKIKP. Vespagrams are calculated using the Phase Weighted Stack [*Schimmel and Paulssen*, 1997]. We then pick the slowness and arrival time of the precursors which are visible.

We determine the location of a precursor, by first backtracing its presumed path through the Earth's interior. A simple ray tracing program calculates raypaths as a function of slowness for 1D earth model AK135. From every point

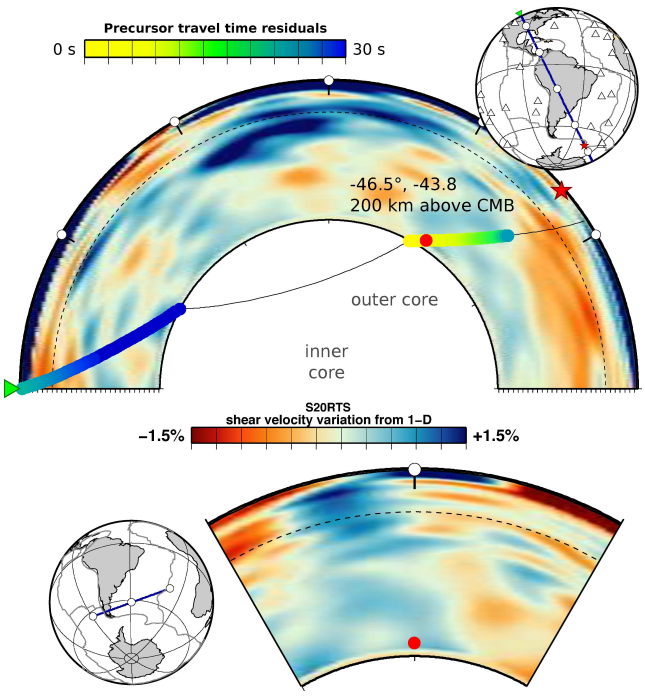

Figure 5. (a) Path of precursor *a* backtraced through the mantle. The colours plotted at every point along the precursor path give the travel time residual between a path from the receiver to that point and on to the source, and the measured precursor travel time. Plotted in the background is mantle tomography model S20RTS (*Ritsema et al.* [1999], *Ritsema et al.* [2004]). (b) cross-section of the mantle near the found precursor location, roughly perpendicular to the direction of subduction of the Nazca plate beneath South America.

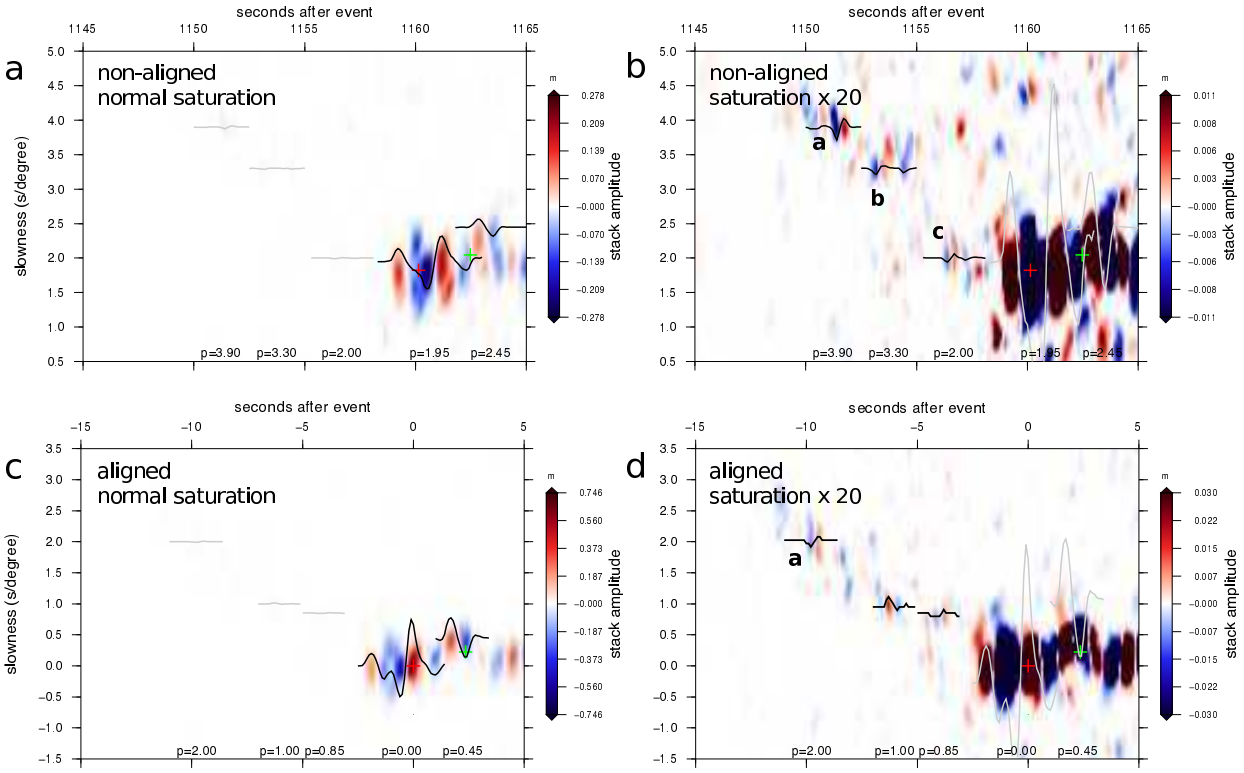

Figure 6. Vespagrams for the precursors to PKIKP for the South Sandwich Islands event of 11 September 2004 ($m_b = 6.1$, depth = 63.9 km). Vespagrams are stacked using the PWS with $\nu = 3$ for paths to North America at epicentral distances of 138-141°. Top figures are from non-aligned (i.e. original) seismograms, bottom figures are from the same set of seismograms but aligned to PKIKP. On the left we see the vespagrams at normal saturation values, on the right the same but with a saturation increased by a factor 20.

along this path, we then calculate the path to the earthquake source and determine the total travel time of the scattered waveform from source to scatterer and from scatterer to receiver. This combined travel time is used to determine the most probable location of the scatterer.

A3. Results

Figure 6 shows the vespagrams for both the non-aligned (Figure 6a,b) and aligned seismograms (Figure 6c,d). The results are very similar, although the different phases are much more defined in the aligned plot, which is much 'cleaner' as well. In the original seismograms, we can distinguish several precursors separately as a result of their coherency across the different traces (see Figure 2). Their amplitudes however, are very small. Indeed the precursors are invisible in a vespagram at normal saturation (Figure 6a,c), where only the phases PKIKP and PKiKP are visible as clear and distinct arrivals.

However, if we increase the saturation levels by a factor 20, the precursors suddenly become visible as a line of arrivals starting at the location of PKIKP and moving away to earlier times and higher slownesses (Figure 6b,d). This is the same pattern that we see in the original seismograms: several precursors arriving increasingly early and at high slowness. Indeed, when we measure the slowness and arrival time in the original seismograms by hand, the results match those from the picked precursors in the vespagrams to within 0.3 s and 0.1 s/°. The phases at high saturation are therefore the same as we see in the vespagrams. Moreover, the waveforms of the different precursors are rather similar, and correspond closely to that of PKIKP. The precursors are more pronounced in the non-aligned plot.

In Figure 6 three precursors are labelled *a*, *b* and *c*. All three have the same polarity as PKIKP. We apply our method to precursor *a*, which is the strongest, and which is clearly the same arrival in both the aligned and non-aligned plots. This precursor has a slowness of 3.90 s/° and arrives at 1151 s after the event origin time.

Figure 5a shows the backtraced precursor path through the mantle. The path goes through the mantle and outer core, and back up towards a point at the surface which is slightly farther away from the receiver than the original source. This is to be expected given the outer core phase slowness and the fact that these rays only arrive at epicentral distances exceeding ∼145°. Travel time residuals for the combined paths are plotted for every point along the ray path. On the receiver side, residuals range from a few to ∼30 seconds, indicating that the scatterer cannot be found in this part of the mantle. At the source side however, there is a clear minimum in travel time residual at (-46.5°, -43.8°), off the coast of Argentina and 200 km above the CMB.

A4. Discussion

Our results indicate that the precursor is situated in the D" layer slightly east of southern South America, in a region with slightly faster velocities than its surroundings (Figure 5a and b). This may be the location of the subducting Nazca slab beneath South America. *Cao and Romanowicz* [2007] associate their precursors with scattering off fossil slabs beneath northwestern North America and a similar mechanism may be at work here. At present this study is too limited to make any further assessment of these structures, but a further study would supply us with more data. In the following paragraphs, we will therefore not comment much on the implications of our results, but more on the method.

The precursors studied here are visible in the seismograms over a range of epicentral distances of at least 3°. This corresponds to ∼65 km lateral distance at the core-mantle boundary, which is significantly larger than the typical wavelength of scatterers derived from global statistical precursor analysis.

We have limited our study to the largest precursor in a set which contains at least two further precursors. Several other arrivals are however visible in the high saturation vespagram, some of which have the same polarity again. We limit ourselves to precursors that are actually visible in the seismograms, because these are by far the most convincing. This does not mean that the other arrivals are random artefacts of the high saturation, and these potentially merit further investigation as well. Interestingly, the precursors are more pronounced in the non-aligned plot than in the plot which is aligned to PKIKP. This may reflect the fact that they have taken a path through the mantle which is significantly different from that of PKIKP, if indeed they are scattered PKPab/bc energy.

The method that we have employed is limited in the sense that we do not explore the full origin direction of the received precursors. However, given the large range of travel time residuals (up to 30 s), a full direction beamforming approach is not likely to move the scatterer location by much. More advanced beamforming techniques could however increase the accuracy of our results. Most of the used seismograms are from the Canadian Northwest Experiment that ran in the years 2003-2005. This array is Y-shaped with arms extending a couple of hundred kilometres in each direction, so that such techniques could potentially be applied with great accuracy.

The setting of our precursor study and that of *Cao and Romanowicz* [2007] is very similar: both study events in the South Sandwich Islands and receivers in northwest Canada. It is then natural to expect that the found precursors are the same or at least close to one another. Yet the results are strikingly different: while their results indicate that all the scatterers are located at the receiver side beneath Canada, ours give a scatterer that is clearly located at the source side.

This could simply be a result of our rudimentary beamforming technique, which does not take into account the back-azimuth of the precursor signal. The largest slowness in *Cao and Romanowicz* [2007] is 3.25 s/°, while our found value is 3.9 s/°. Back-azimuths in *Cao and Romanowicz* [2007] vary from the great-circle path by up to 18°, as a result of which our found slowness may be wrong. A difference in back-azimuth of 20 degrees however only gives a difference in slowness of around 0.25 s/°. Furthermore, apparent slownesses are *minimum* values: the same separation in time has actually been used to travel a shorter distance so the real slowness is higher.

If anything, the actual slowness for our precursor will then be even higher. Even if the slowness is wrong as a result of a wrong back-azimuth, this difference cannot be too large. This is because the original seismograms still show a very regular trend across the traces, while our stations are spread out in all directions over a range of 3°. It is more natural to suppose that we are simply discussing different precursors. The largest precursor in *Cao and Romanowicz* [2007] may simply correspond to another of the precursors in our study, or it is something different altogether.

Our study could be expanded firstly by applying the same method to the other visible precursors. It would be interesting to see whether the origin of lower slowness precursors switches over to the source side, as we see in *Cao and Romanowicz* [2007]. We could also investigate whether precursors are visible in vespagrams of other events. While they are not visible by eye in the original seismograms, they might be hidden in the hugely varying amplitudes, but still present as coherent phases. It would be interesting to see whether other precursors stem from the same source or source region as the precursors that were studied here, or from a different region altogether. To do this accurately, it would be best in all cases to use a full beamforming method which takes the full direction of the signal into account. The very best method to tackle such a problem however, is by calculating the full sensitivity kernel for ther precursors. This is computationally more challenging.

A5. Conclusion

We have found an indication for the presence of scatterers just above the core-mantle boundary. These preliminary results are too rough to draw any firm conclusion, but given the extent of the signals, connections with ancient subduction history are not unlikely. To improve on these results, other precursors should be investigated as well, also taking into account the full direction from which the signal arrives.

Acknowledgments. AD is funded by the European Research Council under the European Community's Seventh Framework Programme (FP7/2007-2013)/ERC grant scheme number 204995. Some parts of NB's research are also supported by this grant. The facilities of the IRIS Data Management System, and specifically the IRIS Data Management Center, were used for access to waveform, metadata or products required in this study. The IRIS DMS is funded through the National Science Foundation and specifically the GEO Directorate through the Instrumentation and Facilities Program of the National Science Foundation under Cooperative Agreement EAR-1063471. Thanks to Arwen Deuss for giving me an awesome opportunity to come to Cambridge. Thanks to Hanneke Paulssen for innumerable good suggestions and discussions and for supervising me 'at home' in Utrecht. Thanks to Jessica Irving, Lauren Waszek, Karen Lythgoe, Paula Koelemeijer, Anna Mäkinen, Chantal van Dinther and Maria Koroni for interesting and helpful discussions. Thanks to my dear papa for reading this the way a lawyer does: nitpickingly. Thanks to my teddy-bear, too.

Notes

1. A separate analysis of the precursors to PKIKP found for this event can be found in Appendix A

References

Bergman, M. I. (1997), Measurements of electric anisotropy due to solidification texturing and the implications for the earth's inner core, *Nature*, *389*(6646), 60–63.

Cao, A., and B. Romanowicz (2007), Locating scatterers in the mantle using array analysis of pkp precursors from an earthquake doublet, *Earth and Planetary Science Letters*, *255*(1), 22–31.

Cormier, V. F. (2007), Texture of the uppermost inner core from forward-and back-scattered seismic waves, *Earth and Planetary Science Letters*, *258*(3), 442–453.

Creager, K. C. (1999), Large-scale variations in inner core anisotropy, *Journal of Geophysical Research: Solid Earth (1978–2012)*, *104*(B10), 23,127–23,139.

Crotwell, H. P., T. J. Owens, and J. Ritsema (1999), The taup toolkit: Flexible seismic travel-time and ray-path utilities, *Seismological Research Letters*, *70*(2), 154–160.

Davies, D., E. Kelly, and J. Filson (1971), Vespa process for analysis of seismic signals, *Nature*, *232*, 8–13.

Deuss, A., J. C. Irving, and J. H. Woodhouse (2010), Regional variation of inner core anisotropy from seismic normal mode observations, *Science*, *328*(5981), 1018–1020.

Doornbos, D., and E. Husebye (1972), Array analysis of pkp phases and their precursors, *Physics of the Earth and Planetary Interiors*, *5*, 387–399.

Hedlin, M. A., P. M. Shearer, and P. S. Earle (1997), Seismic evidence for small-scale heterogeneity throughout the earth's mantle, *Nature*, *387*(6629), 145–150.

Irving, J., and A. Deuss (2011), Hemispherical structure in inner core velocity anisotropy, *Journal of Geophysical Research: Solid Earth (1978–2012)*, *116*(B4).

Jeanloz, R., and H.-R. Wenk (1988), Convection and anisotropy of the inner core, *Geophysical Research Letters*, *15*(1), 72–75.

Karato, S.-i. (1993), Inner core anisotropy due to the magnetic fieldinduced preferred orientation of iron, *Science*, *262*(5140), 1708–1711.

Karato, S.-i. (1999), Seismic anisotropy of the earth's inner core resulting from flow induced by maxwell stresses, *Nature*, *402*(6764), 871–873.

Kennett, B., E. Engdahl, and R. Buland (1995), Constraints on seismic velocities in the earth from traveltimes, *Geophysical Journal International*, *122*(1), 108–124.

Lehmann, I. (1936), P', *Bur. Cent. Seismol. Int. Trav. Sci., A14*, pp. 87–115.

Margerin, L., and G. Nolet (2003), Multiple scattering of high-frequency seismic waves in the deep earth: Pkp precursor analysis and inversion for mantle granularity, *Journal of geophysical research*, *108*(B11), 2514.

Morelli, A., A. M. Dziewonski, and J. H. Woodhouse (1986), Anisotropy of the inner core inferred from pkikp travel times, *Geophysical Research Letters*, *13*(13), 1545–1548.

Niu, F., and L. Wen (2001), Strong seismic scatterers near the core-mantle boundary west of mexico, *Geophysical research letters*, *28*(18), 3557–3560.

Ritsema, J., H. J. van Heijst, and J. H. Woodhouse (1999), Complex shear wave velocity structure imaged beneath africa and iceland, *Science*, *286*(5446), 1925–1928.

Ritsema, J., H. J. van Heijst, and J. H. Woodhouse (2004), Global transition zone tomography, *Journal of Geophysical Research: Solid Earth (1978–2012)*, *109*(B2).

Schimmel, M., and H. Paulssen (1997), Noise reduction and detection of weak, coherent signals through phase-weighted stacks, *Geophysical Journal International*, *130*(2), 497–505.

Shearer, P. M. (1994), Constraints on inner core anisotropy from pkp (df) travel times, *Journal of Geophysical Research: Solid Earth (1978–2012)*, *99*(B10), 19,647–19,659.

Song, X., and D. V. Helmberger (1995), Depth dependence of anisotropy of earth's inner core, *Journal of Geophysical Research: Solid Earth (1978–2012)*, *100*(B6), 9805–9816.

Song, X., and X. Xu (2002), Inner core transition zone and anomalous pkp (df) waveforms from polar paths, *Geophysical research letters*, *29*(4), 1042.

Sun, X., and X. Song (2008), Tomographic inversion for three-dimensional anisotropy of earths inner core, *Physics of the Earth and Planetary Interiors*, *167*(1), 53–70.

Tanaka, S., and H. Hamaguchi (1997), Degree one heterogeneity and hemispherical variation of anisotropy in the inner core from pkp (bc)–pkp (df) times, *Journal of geophysical research*, *102*(B2), 2925–2938.

Thomas, C., J. Kendall, G. Helffrich, et al. (2009), Probing two low-velocity regions with pkp b-caustic amplitudes and scattering, *Geophysical Journal International*, *178*(1), 503–512.

Waszek, L., and A. Deuss (2011), Distinct layering in the hemispherical seismic velocity structure of earth's upper inner core, *Journal of Geophysical Research: Solid Earth (1978–2012)*, *116*(B12).

Wen, L. (2000), Intense seismic scattering near the earth's core-mantle boundary beneath the comoros hotspot, *Geophysical research letters*, *27*(22), 3627–3630.

Woodhouse, J. H., D. Giardini, and X.-D. Li (1986), Evidence for inner core anisotropy from free oscillations, *Geophysical Research Letters*, *13*(13), 1549–1552.